JOURNAL OF OPTOELECTRONICS AND ADVANCED MATERIALS Vol. 9, No. 6, June 2007, p. 1904 - 1910

Synthesis and settings behavior of α-TCP from calcium deficient hyroxyapatite obtained by hydrothermal method

B. JOKIC, I. JANKOVIC-CASTVAN, DJ. VELJOVIC, D. BUCEVAC[a],
K. OBRADOVIC-DJURICIC[b],R. PETROVIC, DJ. JANACKOVIC[*]
Faculty of Technology and Metallurgy, Karnegijeva 4, 11000 Belgrade, Serbia
[a]*Institute for Nuclear Science, Vinca, Belgrade, Serbia*
[b]*Faculty of Stomatology, Belgrade, Serbia*

The aim of this work is the investigation of alpha-tricalcium-phosphate (α-TCP) formation from calcium-deficient hydroxyapatite (CDHAP), synthesized by hydrothermal method from $CaCl_2$, EDTA, $NaH_2PO_4 \cdot 2H_2O$ and urea as precursors at 160 ^oC. Further, the influence of Ca/P ratios in the starting solution on α-TCP formation and the settings of obtained cements in simulated body fluid (SBF) were investigated. According to the results of X-ray, FTIR and SEM analyses, it is shown that CDHAP is transformed to β-TCP at 800 ^oC, and to α-TCP at 1200 ^oC. Almost complete transformation of CDHAP into α-TCP occur after heating at 1500 ^oC in the case when Ca/P ratio in starting solution was 1,42. Cement powder mixed with the cement liquid (2.5 wt.% solution of Na_2HPO_4) completely hydrolyzes after 7 days in SBF, forming only CDHAP phase.

(Received March 23, 2007; accepted April 26, 2007)

Keywords: α-TCP Cements, Synthesis, Calcium Deficient Hydroxyapatite

1. Introduction

Development of calcium phosphate cements (CPC) as a class of viable biomaterials has increased interest since 1980s, as substitutes for bone tissues and as a fixation material between ceramics and natural bone tissues in clinical applications such as orthopedic, reconstructive, oral and maxillofacial surgery [1]. There are significant advantages in application of these cements since they self-setting under ambient or human body temperature, offer the surgeon moldability, injectability, complete filling of a cavity within the operating theatre and suitable mechanical strength in acceptable clinical time [2]. Further advantage of CPCs is that they do not exhibit dimensional change or any detectable thermal effect [3,4], neither exothermic nor endothermic. CPC activate function of osteoblast in the development of new bone, while simultaneously being resorbed by osteoclast as a part of lifelong orderly process of the bone remodeling.

Brown and Chow [5] first reported the formation of the apatite cement consisting of a mixture of tetracalcium phosphate (TTCP) and dicalcium phosphate anhydride (DCPA) or dicalcium phosphate dihydrate (DCPD) as a solid phase. From that time, a number of investigations of synthesis, setting and mechanical properties of various type of CPC, have been reported [6-13]

One of the most interesting CPC is α-TCP, which is more soluble than hydroxyapatite (HAP) due to its hydrolysis in aqueous solution and settings through the mechanisms according to the following reaction

$$3Ca_3(PO_4)_2 + H_2O \rightarrow Ca_9(HPO_4)(PO_4)_5OH$$

This reaction, first described by Monma and Kanazawa [14], implies progressive dissolution of α-TCP particles and successive precipitation of a more stable phase. The products of hydrolysis can be octacalcium phosphate ($Ca_8H_2(PO_4)_6.5H_2O$), CDHAP or HAP, depending on the synthesis conditions [15-17].

Many kind of precursors have been used for preparation of α-TCP based cements, for example mixture of α-TCP (produced by solid state reaction of equimolar mixture of calcium hydrogen phosphate and calcium carbonate) with monocalcium phosphate monohydrate (MCPM) and CaO [18], DCPD and $Ca(OH)_2$, $CaCO_3$ [19] or $CaHPO_4$ [9] etc. Doi et al. [20] reported that carbonate apatite, synthesized by the conventional wet methods, is slightly decomposed after heating at 1500^{o}C into tetracalcium phosphate (TTCP) and α-TCP with the major phase still being apatite. According to Raynaud et al. [21], HA powders, obtained by aqueous precipitation method, with Ca/P < 1.50, are transformed into α-TCP at 1250^{o}C while HA powder with Ca/P = 1.535 are decomposed into α-TCP and stoichiometric HA after heating at 1300^{o}C. More stable at higher temperatures is HA powder with Ca/P = 1.667.

The aim of this work is investigation of the α-TCP synthesis from CDHAP, obtained by hydrothermal method from $CaCl_2$, EDTA, $NaH_2PO_4 \cdot 2H_2O$ and urea as precursors at 160^{o}C. The influence of Ca/P ratio in the starting solution on α-TCP formation as well as phase and

microstructural changes during setting of these cement by immersion in SBF were investigated by FTIR, X-ray and SEM analyses.

2. Experimental Procedure

2.1 Synthesis of calcium deficient hydroxyapatite:

Synthesis of CDHAP particles was performed according to method described earlier elsewhere [22-24]. The various amounts of $CaCl_2$, $Na_2H_2EDTA{\cdot}2H_2O$, NaH_2PO_4 and urea were dissolved in 2000 ml of distilled water (see Table 1.). All reagents were Merck p.a. grade. The solution was heated at 160°C during 3 h in a sealed tube. The particles were further washed with distilled water and dried at 105°C for 2 h.

Table 1. The precursor contents(in 2000 ml distilled water) for CDHAP synthesis.

	$CaCl_2{\cdot}2H_2O$ (g)	$Na_2H_2EDTA{\cdot}2H_2O$ (g)	$NaH_2PO_4{\cdot}2H_2O$ (g)	$CO(NH_2)_2$ (g)
HAP1 (Ca/P=0.97)	11.00	14.80	12.00	12.00
HAP2 (Ca/P=1.42)	15.96	14.80	12.00	12.00
HAP3 (Ca/P=1.67)	18.86	14.80	12.00	12.00

2.2 Synthesis of α-$Ca_3(PO_4)_2$ cement:

The α-$Ca_3(PO_4)_2$ cement was obtained by heating of dried HAP1, HAP2 and HAP3 powders at heating rate of 10°C/min and calcinations at 800, 1200 and 1500°C during 2 hours. The heated samples were milled in vibratory mill (Fritsch, Germany) with WC disc, during 3 minutes. Obtained cement powders C1, C2 and C3 were further mixed with phosphate solution (2.5 wt.% solution of Na_2HPO_4) at a liquid to powder ratio of 0.32 ml/g [25] in order to obtain the cement paste CP1, CP2 and CP3, respectively. These pastes were molded in cylindrical shape, and after 30 minutes were immersed in simulated body fluid (SBF) for 1, 2, 7 and 14 days.

2.3 Characterization methods:

X-ray diffraction analyses were performed on Siemens Crystalloflex, D-500 diffractometer with CuKα1 radiation and a graphite monochromator, with the range angle 2θ from 20-50° and step width 0.02. FTIR analyses were conducted on MB Bomen 100 Hartmann and Braun spectrometer in the wavenumber range from 400 to 4000 cm^{-1}. The samples were prepared by the KBr method at a ratio sample: KBr=1:150. The morphology of samples was examined by scanning electron microscopy with a Jeol T-20 microscope. Ca/P molar ratio of samples were examined by chemical analysis using ICP ACP Spectro Ciros Vision.

3. Results and discussion

The micrographs of spherical nonagglomerated particles, obtained by hydrothermal method are shown in the Fig. 1. It could be seen that particle with size is in the range of 2 to 4 μm are obtained. Increase of the Ca/P ratio in the staring solutions resulted in the some increasing of the particle size. The particles consist of large number of aggregated rod-like nanoparticles with size around 100 nm. It can be also observed that the particles synthesized at lower Ca/P ratio show a non uniform morphology with sharp needle-like crystals on the surface (Fig. 1a), while particles synthesized from solution with higher Ca/P ratio exhibit uniform morphology with surface composed of smaller crystallites.

The micrograph of HAP2 particles milled after annealing at 1500 °C, is presented visible in Fig. 2. It can be observed that the particles have a microstructure typical for milled solid-state product with particle diameter ranging from 0.5 to 7 μm.

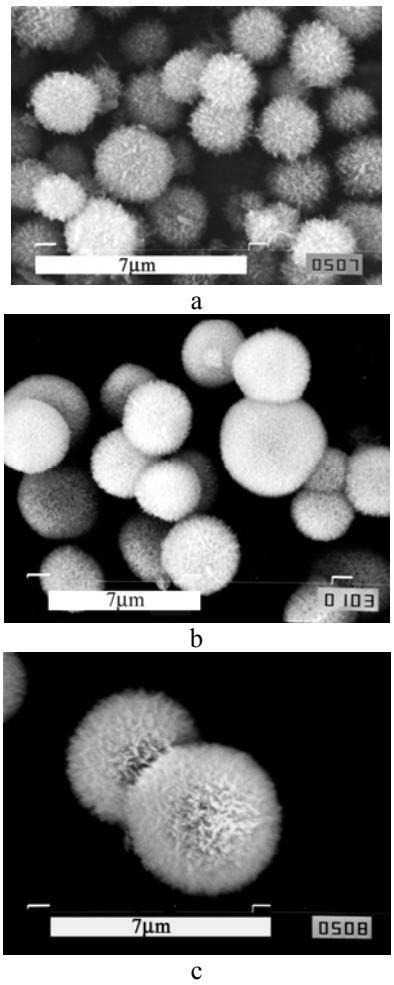

Fig. 1. SEM micrographs of the CDHAP particles obtained by hydrothermal method: a) HAP1, b) HAP2, c) HAP3.

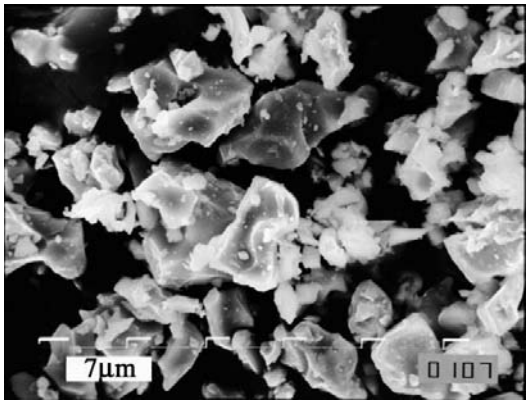

Fig. 2. SEM micrographs of HAP2 powder heated at 1500°C and milled.

The XRD spectrum of the synthesized powders is shown if Figure 3. It can be seen that there is no significant difference between peaks of samples synthesized at various starting Ca/P ratios. HAP phase are partially transformed in the α-TCP phase after heating of the HAP1, HAP2 and HAP3 samples at 1500°C for 2h (Fig. 4). The X-ray diffraction patterns show that only HAP2 powder transforms almost completely to α-TCP, while HAP1 and HAP3 powder still preserve appreciable amount of CDHAP phase. The phase transformation of the HAP2 sample heated at 800, 1200 and 1500 °C, respectively, is shown in Fig. 5. From these diffractograms it can be seen that at 800°C, synthesized CDHAP partially transforms to β-TCP, which is further transformed to α-TCP after heating at 1200°C. It was observed that at 800 °C, besides the newly formed β-TCP, phase CDHAP phase is still present, suggesting that CDHAP do not transform completely into β-TCP. It is also observed that by increasing the heating temperature for CDHAP samples, a large amount of α-TCP phase was obtained, as indicated by comparation of the XRD peaks intensity for α-TCP and CDHAP. It was earlier found that non-stoichiometric apatite with formula $Ca_{10-x}(OH)_{2-x}$ $(HPO_4)_x(PO_4)_{6-x}$ ($0 \leq x \leq 1$) have a similar XRD spectrum, despite its Ca/P molar ratio being 1.67, 1.5 or between 1.67 and 1.5. This non-stoichiometric apatite transforms by heating completely in β-TCP only when the Ca/P ratio is 1.5, that corresponds to $Ca_9(HPO_4)(PO_4)OH$ [26]. In the case of the sample HAP2 with further heating at 1200°C for 2h, appreciably amount of CDHAP was observed, while at 1500 °C for 2h, only small amount of residual CDHAP phase is present (Fig. 5.)

The crystalline phase identified by X-ray diffraction analysis in the CP2 cement paste after different periods of soaking in SBF is shown in Fig.6. It could be seen that after two days of hydratation at 37°C, the α-TCP partially transform in the CDHAP. The intensities of the diffraction peaks characteristic for apatite increase with prolonged soaking time, while the intensity of α-TCP peaks decreases. The diffraction peaks characteristic for α-TCP are no longer observed in the patterns recorded after 7 day of aging in SBF.

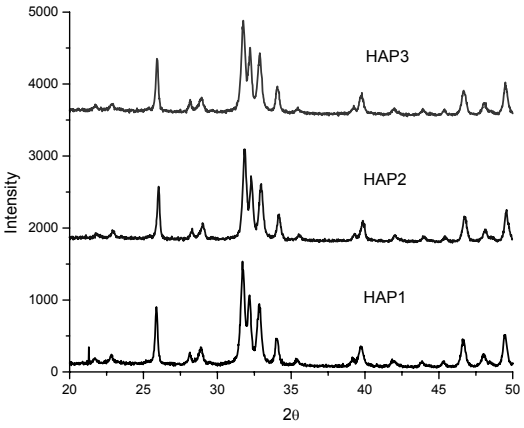

Fig. 3. X-ray diffractograms of HAP1, HAP2 and HAP3 powder dried at 105°C.

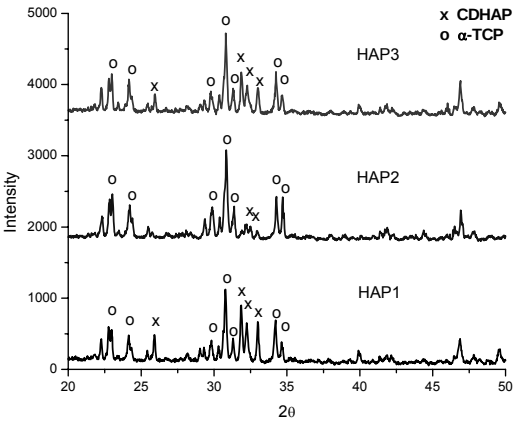

Fig. 4. X-ray diffractograms of HAP1, HAP2 and HAP3 powder annealed at 1500°C.

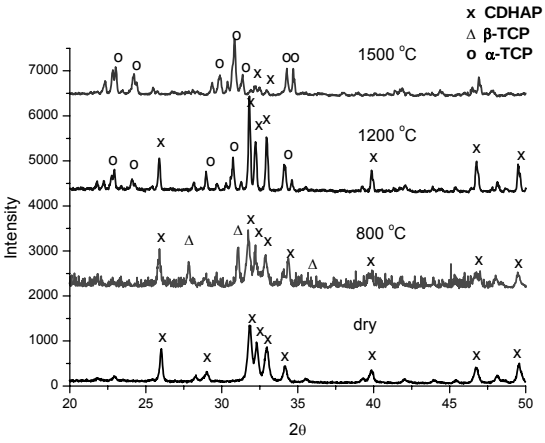

Fig. 5. X-ray diffractograms of the HAP2 powder heated at 800, 1200 and 1500°C for 2h.

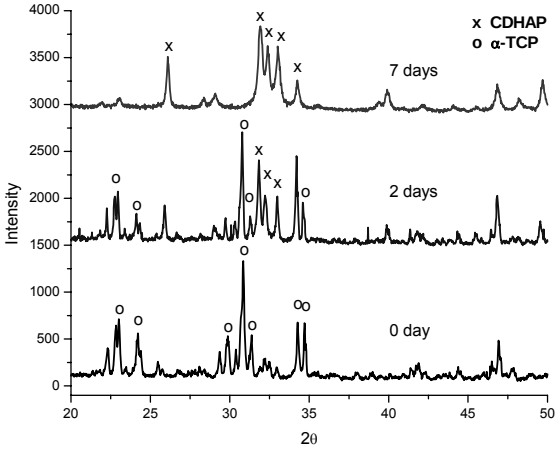

Fig. 6. X-ray diffractograms of C2 samples heated at 1500°C after immersion in SBF for 0, 2 and 7 days.

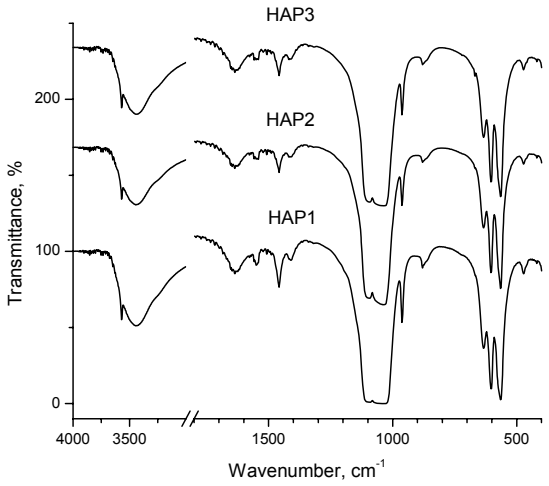

Fig. 7. FTIR spectra of HAP1, HAP2 and HAP3 samples dried at 105°C.

The FTIR spectra of the synthesized and dried at 105 °C HAP1, HAP2 and HAP3 powders are shown in Fig. 7. The characteristic bands of phosphate group at 470, 567, 601, 962 and 1040-1125 cm^{-1} are present in the spectrum of the dried samples. The bands appearing at wave number of 873, 1420 and 1480 cm^{-1} are a consequence of the carbonate ion incorporation in the apatite structure. The peak intensity of the bands corresponding to carbonate ion group decrease with increasing heating temperature, from 105 to 1500°C. Appearance of the bands at 877 cm^{-1} of the dried and annealed at 800 °C samples indicates the presence of HPO_4^{2-} groups that are overlapped with band at 873 cm^{-1} arised from CO_3^{2-} group [26,27].

The broad bands observed at 1650 and 3440 cm^{-1} indicate adsorbed H_2O in the materials. The adsorbed water band at around 3440 cm^{-1} overlaps with the weak bands at around 3565 cm^{-1}, which corresponds to structural OH, and these are not clearly visible at samples heated at 1500 °C. The band at 3744 cm^{-1} is assigned to O-H stretch. The band due to structural OH group in HAP also occurs at around 633 cm^{-1} [26,27]. Further heating of HAP1, HAP2 and HAP3 samples at 800°C, develops the band at 1191 cm^{-1} in FTIR spectra (Fig. 8.) which corresponds to $P_2O_7^{4-}$ group, as a consequence of HPO_4^{2-} ions condensation in CDHAP ($2HPO_4^{2-} \rightarrow P_2O_7^{4-} + H_2O$), could be also observed [28]. After heating the samples at 1500°C (Fig. 9) the disappearance of bands at 877 and 873 cm^{-1} that corresponding HPO_4^{2-} and CO_3^{2-} group, respectively, were observed.

The FTIR analysis of the cement immersed in SBF is shown in Fig.10. It could be seen that bands at 877 cm^{-1} and the weak shoulder at 1215 cm^{-1} (characteristic of HPO_4^{2-} groups) and at 633 cm^{-1} (which correspond to OH groups) appear in the sample after settings in SBF during 7 days (Fig. 10.) indicating that the CDHAP phase with composition $Ca_{10-x}(HPO_4)_x(PO_4)_{6-x}(OH)_x$, is formed [28].

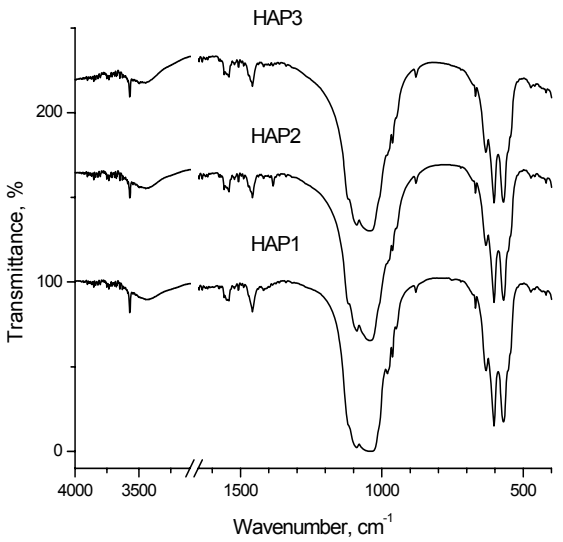

Fig. 8. FTIR spectra of HAP1, HAP2 and HAP3 samples annealed at 800°C.

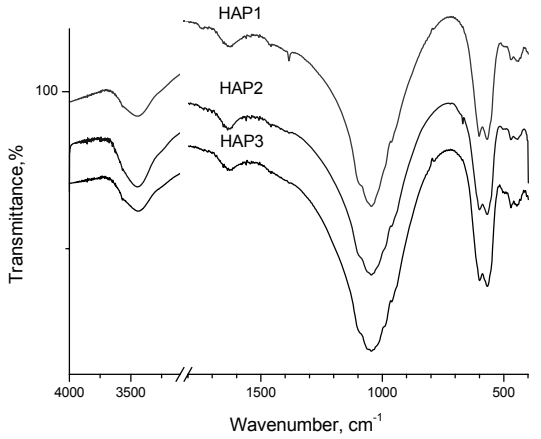

Fig. 9. FTIR spectra of HAP1, HAP2 and HAP3 samples annealed at 1500°C.

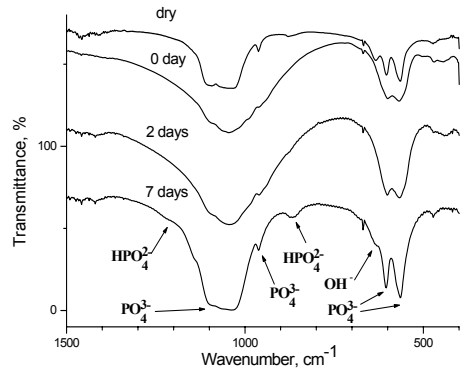

Fig. 10. FTIR spectra of dried HAP2, annealed at 1500 °C and after setting in SBF for 2 and 7 days.

Evolution of the microstructure of CP1, CP2 and CP3 cements, prepared from mixture of α-TCP and a solution 2,5 wt.% of Na_2HPO_4, before (0 day) and after setting of samples in simulated body fluid at 37 °C for 1, 2 and 14 days, was observed by SEM and shown in Figs. 11, 12 and 13.

Microstructural evolution of new CDHAP phase on CP2 sample is clearly visible after 1 day (see Fig. 12.b) compared with the CP1 and CP3 samples (Fig. 11b, and Fig. 13b), where the formation of the new phase on starting particles surface after the same period of immersion was not clearly observed. It can be also seen that the small needle-like crystals are occasionally formed on the cement particles, but the cement particles are still visible at micrographs of CP1 and CP3 sample (Fig.11b and 13b).

The micrograph of CP1 sample after 2 days of immersion in SBF (Fig. 11c), shows that the particles surface is covered by nanosized crystallites of precipitated CDHAP, but presence of the voids between primary particles is still visible. After the same time of immersion of CP2 sample in SBF (Fig. 12c), well developed structure of newly formed CDHAP phase, with high degree of interconnectivity between primary α-TCP particles, is observed. It is in accordance with decreasing of the XRD peaks intensity of α-TCP (Fig. 6) with time and appearing forming developing of hydroxyapatite phase after 2 day. Microstructure of the CP3 sample show the lower degree of changes (Fig. 13c), comparing with microstructures of the CP1 and CP2 samples after the same period of immersion (Fig. 11c and 12c), suggesting that the hydrolysis reaction of α -TCP do not occurred in all samples at the same rate. Although the surface of the starting CP2 particles cannot be observed due to the fact that well defined needle like CDHAP nanoparticles are formed at the surfaces, the X-ray diffractogram of the same sample (Fig. 6.) indicates that a significant amount of α-TCP phase is still present. Even thought the α-TCP particles appear to be isolated from the solution by newly formed apatite phase, it seems that needle-like crystallites network is still porous allowing the ions transport without retarding the process of hydrolysis. From the same micrographs it could be seen that the surface of the cement particles still shows the presence of pores.

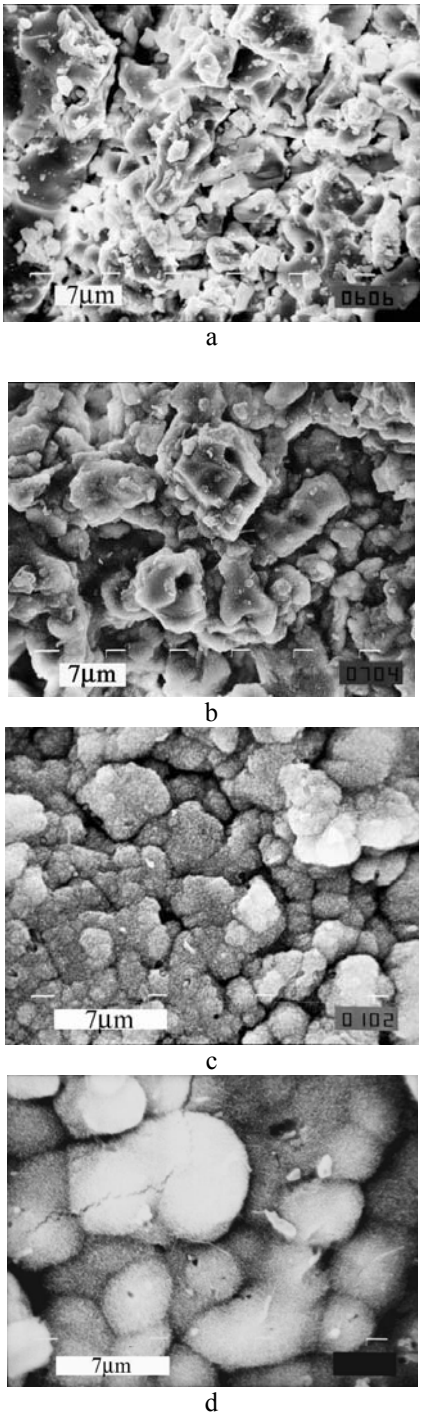

Fig. 11. SEM micrographs of the surface of CP1 cement samples soaked for a) 0, b) 1 c) 2 and d) 14 days in SBF.

The micrographs of CP1 and CP2 samples after 14 days of immersion in SBF, presented in Fig. 11d and 12d, suggest that complete hydrolysis of α-TCP has occurred, with visible denser microstructures. The starting cement particles cannot be observed, what is confirmed also by completely disappearing of α-TCP phase on diffractogram in Fig. 6. As the setting reaction proceeds, the structures became denser and the surfaces become largely covered with entangled nanocrystals of CDHAP that grow on cement particles surface. In the case of CP3 samples, the microstructure after 1, 2 and 14 days of immersion shows

the lowest changes compared with the CP1 and CP2 samples. This can be explained by the lower α-TCP/HAP ratio in starting CP3 cement powder. Further, comparing the samples after immersion in SBF for 14 days (Figs. 11d, 12d, 13d) it can be also observed that the CP2 sample have the densest microstructure with finer nanostructure and smaller size of newly formed CDHAP crystals. This can be explain by the higher content of α-TCP in the case of C2 cement, where more Ca^{2+} and PO_4^{3-} ions could be obtained during hydrolysis, increasing the ions concentration in shorter time and enabling more nucleus of CDHAP to be formed at the surface of the particles.

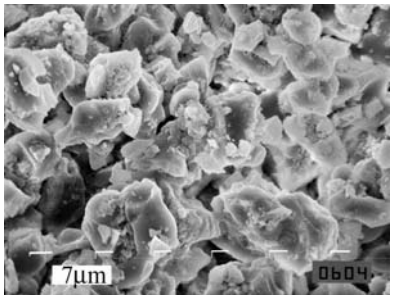

a

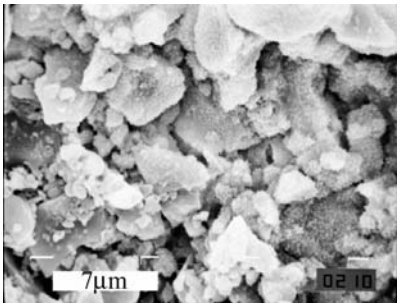

b

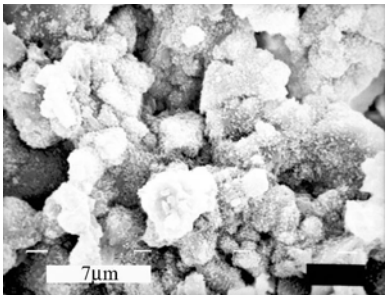

c

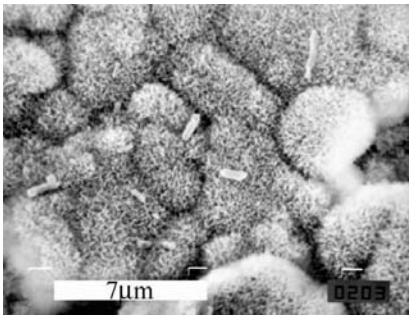

d

Fig. 12. SEM micrographs of the surface of CP2 cement samples soaked for a) 0, b) 1, c) 2 and d) 14 days in SBF.

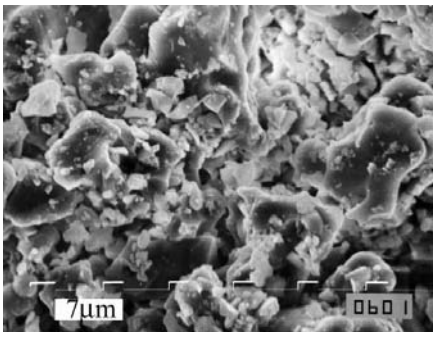

a

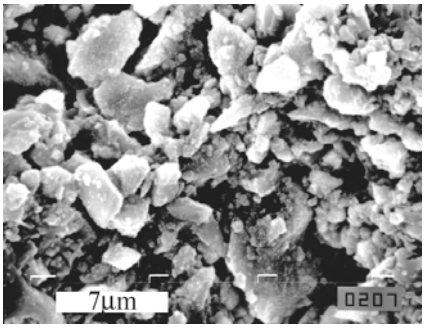

b

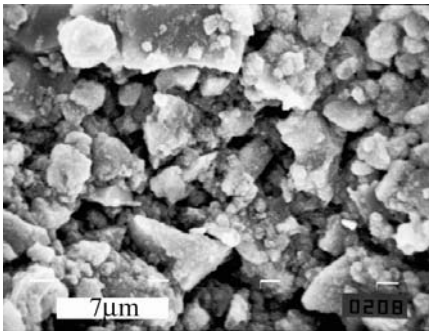

c

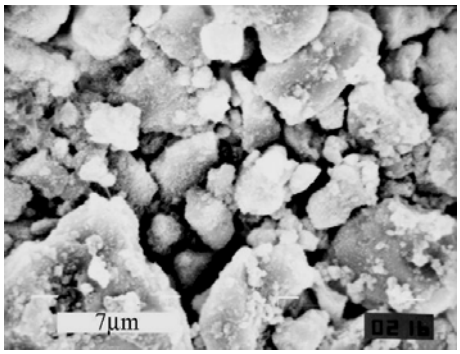

d

Fig. 13. SEM micrographs of the surface of CP3 cement samples soaked for a) 0, b) 1, c) 2 and d) 14 days in SBF.

4. Conclusion

According to the results of X-ray and FTIR analyses it can be concluded that synthesized HAP powders are transformed to β-TCP at 800 ^{o}C, and to α-TCP at 1200^{o}C.

CDHAP synthesized from solutions with different starting Ca/P ratio leads to the formation of various amount of α-TCP phase after heating at different temperatures. Almost complete transformation of CDHAP into α-TCP occur after heating at 1500 ^{o}C in the case when Ca/P ratio in HAP powder was 1,56.

Cement pastes prepared from cement powders with various α-TCP/CDHAP ratios indicate different setting behavior during immersion in SBF, caused by various amount of α-TCP phase. The cement paste prepared from cement powder with higher amount of α-TCP phase exhibits the more compact and denser microstructure with the finer nanostructure and smaller size of newly formed CDHAP.

Acknowledgement

The authors wish to acknowledge the financial support from the Ministry of Science and Technology Republic of Serbia through the projects No 142070B and EUREKA E! 3033 Bionanocomposit. This work was presented at the Workshop of EUREKA Project E! 3033, which was held in Bucharest and Sinaia, Romania, January 2006.

References

[1] K. Takahashi, Y. Fujishiro, S. Yin, T. Sato, Ceram. Inter. **30**, 199 (2004).
[2] E. Fernandez, F. J. Gil, M. P. Ginebra, F. C. M. Driessens, J. Mater. Sci. Meter. Med. **10**, 169 (1999).
[3] I. Khairoun, F. C. M. Driessens, M. G. Boltong, J. A. Planell, R. Wenz, Biomaterials **20**, 393 (1999).
[4] Y. Miyamoto. K. Ishikawa, H. Fukao, M. Sawada, M. Nagayama, M. Kon, K. Asaoka, Biomaterials **16**, 855 (1995).
[5] P. W. Brown, N. Hocker, S. Hoyle, J. Amer. Ceram. Soc. **74**, 1848 (1991).
[6] L. Yubao, Z. Xingdong, K. de Groot, Biomaterials **18**, 737 (1997).
[7] M. Watanabe, M. Tanaka, M. Sakurai, M. Maeda, J. Europ. Ceram. Soc. **26**, 549 (2006).
[8] E. Fernandez, F. J. Gil, M. P. Ginebra, F. C. M. Driessens, J. A. Planell, J. Mater. Sci. Meter. Med, **10**, 223 (1999).
[9] Q. Yang, T. Troczynski, D. M. Liu, Biomaterials **23**, 2751 (2002).
[10] A. Almirall, G. Larrecq, J.A. Delgado, S. Martinezb, J. A. Planell, M. P. Ginebra, Biomaterials **25**, 3671 (2004).
[11] D. Walsh, J. Tanaka, J. Mater. Sci. Meter. Med. **12**, 339 (2001).
[12] K. Ishikawa, S. Takagi, L. C. Chow, K. Suzuki, J. Biomed. Mater. Res. **46**, 504 (1999).
[13] F. C. M. Driessens, M. G. Boltong, E. A. P. de Maeyer, R. Wenz, B. Nies, J. A. Planell, Biomaterials **23**, 4011 (2002).
[14] H. Monma, S. Uenoso, T. Kanazawa, J. Chem. Technol. Biol. **31**, 15 (1981).
[15] C. Durucan, P. W. Brown, J. Mater. Sci. Mater. Med. **11**, 365 (2000).
[16] A. Bigi, E. Boanini, R. Botter, S. Panzavolta, K. Rubini, Biomaterials **23**, 1849 (2002)
[17] K. S. TenHuisen, P. W. Brown, Biomaterials **19**, 2209 (1998).
[18] O. Bermudez, M. G. Boltong, F. C. M. Driessens, J. A. Planell, J. Mater. Sci. Mater. Med. **5**, 160 (1994).
[19] S. Takagi, L. C. Chow, K. Ishikawa, Biomaterials **19**, 1593 (1998).
[20] Y. Doi, Y. Shimizu, Y. Moriwaki, M. Aga, H. Iwanaga, T. Shibutani, K. Yamamoto, Y. Iwayama, Biomaterials **22**, 847 (2001).
[21] S. Raynaud, E. Champion, D. Bernache-Assollant, P. Thomas, Biomaterials **23**, 1065 (2002).
[22] Dj. Janackovic, I. Petrovic-Prelevic, Lj. Kostic-Gvozdenovic, R. Petrovic, V. Jokanovic, D. Uskokovic, Key Engin. Mater. **192-195**, 203 (2001).
[23] Dj. Janackovic, I. Jankovic, R. Petrovic, Lj. Kostic-Gvozdenovic, S. Milonjic, D. Uskokovic, Key Engin. Mater. **240-242**, 437 (2003).
[24] B. Jokic, I. Jankovic-Castvan, Dj. Veljovic, R. Petrovic, S. Drmanic, Dj. Janackovic, Key Engin. Mater. **309-311**, 821 (2006).
[25] M. P. Ginebra, M. G. Boltong, E. Fernandez, J. A. Planell, F. C. M. Driessens, J. Mater. Sci. Mater. Med. **6**, 612 (1995)
[26] A. Stoch, W. Jastrzebski, A. Brozek, J. Stoch, J. Szaraniec, B. Trybalska, G. Kmita, J. Mol. Struct. **555**, 375 (2000).
[27] R. N. Panda, M. F. Hsieh, R. J. Chung, J. Phys. Chem. Solids **64**, 193 (2003).
[28] F. H. Lin, C. J. Liao, K. S. Chen, J. S. Sun, Biomaterials **19**, 1101 (1998).

*Corresponding author: nht@tmf.bg.ac.yu;
nht@elab.tmf.bg.ac.yu